A Letters Journal Exploring the Frontiers of Physics

May 2012

EPL, **98** (2012) 44003
doi: 10.1209/0295-5075/98/44003

www.epljournal.org

# Ultrasolitons: Multistability and subcritical power threshold from higher-order Kerr terms

David Novoa[1(a)], Daniele Tommasini[2] and Humberto Michinel[2]

[1] *Centro de Láseres Pulsados Ultracortos Ultraintensos (CLPU) - Plaza de la Merced s/n, Salamanca, ES-37008 Spain, EU*
[2] *Departamento de Física Aplicada, Universidade de Vigo - As Lagoas s/n, Ourense, ES-32004 Spain, EU*

received 10 January 2012; accepted in final form 17 April 2012
published online 17 May 2012

PACS 42.65.Tg – Optical solitons; nonlinear guided waves
PACS 42.65.Jx – Beam trapping, self-focusing and defocusing; self-phase modulation
PACS 42.65.Pc – Optical bistability, multistability, and switching, including local field effects

**Abstract** – We show that an optical system involving competing higher-order Kerr nonlinearities can support the existence of *ultrasolitons*, namely extremely localized modes that only appear above a certain threshold for the central intensity. Such new solitary waves can be produced for powers *below* the usual collapse threshold, but they can also coexist with ordinary, lower-intensity solitons. We derive analytical conditions for the occurrence of multistability and analyze the dynamics of the different kinds of fundamental eigenmodes that can be excited in these nonlinear systems. We also discuss the possible transitions between solitary waves belonging to different nonlinear regimes through the mechanism of soliton switching.



**Introduction.** – A recent measurement of the instantaneous higher-order Kerr (HOKE) coefficients in gases [1] has led to a revolutionary description of the filamentation of ultrashort laser pulses [2]. The filament stabilization is attributed to the competition of the HOKE focusing and defocusing contributions to the refractive index alone, rather than to their interplay with the ionization-induced plasma defocusing, which had a key role in the traditional interpretation [3]. This new paradigm has stimulated an increasing amount of work [4–11], aimed either at testing the controversial results reported in refs. [1,2], or at the theoretical exploration of its rich phenomenological implications [12–17].

In this letter, we will demonstrate that, within a well-defined parameters region, a system involving just local HOKE nonlinearities can support the existence of a new branch of localized solutions that will be called *ultrasolitons*. Such stationary states coexist with solitons of lower intensity, similar to those found for common optical media [12]. Very remarkably, this implies the emergence of *optical soliton multistability* (OSM), *i.e.* the existence of two or more stationary states with the same power and different propagation constants and profiles, like in the systems reported in refs. [18–21] and in the recent work [22], that has appeared while we were preparing the revised version of the present paper. We will also derive an analytical condition on the HOKE coefficients for the emergence of OSM, and show that the ultrasolitons can be *subcritical*, *i.e.* they may exhibit powers even below the ordinary collapse threshold [23]. Finally, we will discuss the transitions among multistable states through efficient *soliton switching* processes.

**Mathematical model.** – Let us consider a wave system evolving along the $\eta$ direction in the space of transverse coordinates $\xi$ and $\chi$, and assume that the complex wave function $\Psi(\xi,\chi,\eta)$ satisfies the (dimensionless) nonlinear Schrödinger equation

$$i\frac{\partial\Psi}{\partial\eta}+\frac{1}{2}\nabla_\perp^2\Psi+F(|\Psi|^2)\Psi=0, \tag{1}$$

where $\nabla_\perp^2=\partial^2/\partial\xi^2+\partial^2/\partial\chi^2$ and

$$F(|\Psi|^2)=\sum_q(-1)^{q+1}f_{2q}|\Psi|^{2q}. \tag{2}$$

This formalism applies to the paraxial propagation of the linearly polarized electric field $E(x,y,z)$ of a laser pulse of mean wave number in vacuum $k_0=2\pi/\lambda_0$, being $\lambda_0$ the central wavelength, in a nonlinear optical medium whose refractive index depends upon the intensity $I=\epsilon_0 cE^2$

(a) E-mail: dnovoa@clpu.es

as $n = n_0 + \Delta n = n_0 + \sum_{q=1}^{4} n_{2q} I^q$. In fact, motivated by the results of ref. [1] for the optical response of common gases, we will assume that the refractive index involves 4 terms of increasing powers in the intensity $I$ of the beam, with alternating sign coefficients $n_2, n_6 > 0$ and $n_4, n_8 < 0$, that contribute to focusing and defocusing respectively. We will choose the dimensionless quantities such that $f_2 = f_4 = 1$. The relations between the dimensional and dimensionless physically relevant quantities are then $(\xi, \chi) = (n_0/|n_4|)^{1/2}(k_0 n_2)(x, y)$, $\eta = (k_0 n_2^2/|n_4|)z$, $\Psi(\xi, \chi, \eta) = (\epsilon_0 c|n_4|/n_2)^{1/2} E(x, y, z)$, $\Delta n = (n_2^2/|n4|)F$, $n_6 = (n_4^2/n2) f_6$ and $n_8 = (n_4^3/n2^2) f_8$. The only free parameters included in eq. (1) are then $f_6$ and $f_8$, that will be assumed to be positive.

For the sake of clarity, and motivated by refs. [1,2,12], in this letter we will neglect the effects of multiphoton absorption, ionization and temporal dispersion of the optical pulses. However, we emphasize that our results may also be applied to multilevel atomic media, where the dependence of $\Delta n$ given by eq. (2) may be achieved by the coherent control of the atomic ensemble via quantum-engineering techniques [24].

**Analytical condition for multistability.** – Let us now derive an analytical condition for the possible emergence of OSM. Assuming radial symmetry, we search for soliton solutions of the form $\Psi(\xi, \chi, \eta) = \Phi(r) e^{-i\mu\eta}$, where $r \equiv \sqrt{\xi^2 + \chi^2}$ and $\mu$ is the propagation constant. As discussed in refs. [12,25], $\mu$ can be identified with the chemical potential of an equivalent thermodynamical 2D system of $N = \int \rho \mathrm{d}\xi \mathrm{d}\chi \equiv \int |\Phi|^2 \mathrm{d}\xi \mathrm{d}\chi$ particles (for the optical system, $N = n_0 k_0^2 n_2 \mathcal{P}$ , where $\mathcal{P}$ is the total power of the optical field). Equation (1) can then be derived by minimizing the Landau's grand potential [26] $\Omega = -\int p \mathrm{d}\xi \mathrm{d}\chi$, where the pressure field $p$ is

$$p = -\frac{1}{2}|\nabla_\perp \Phi|^2 + \mu|\Phi|^2 + \int_0^{|\Phi|^2} F(U)\mathrm{d}U. \qquad (3)$$

In particular, assuming the dependence given in eq. (2), the integral term in eq. (3) can be written as $\sum_q (-1)^{q+1} \frac{f_{2q}}{q+1} |\Phi|^{2(q+1)}$.

In the case of a high-power solution with a flat-top profile of radius $R$, calling $A = \Phi(0)$ the amplitude of the large and homogeneous central region, eq. (1) implies

$$\mu = -F(A^2), \qquad (4)$$

where we choose the arbitrary phase of the solution such that $A$ is positive real. On the other hand, as shown in refs. [12,25], any such flat-top solitons obey the Young-Laplace (YL) equation [26], $p_c = 2\sigma/R$, where $R$ is the radius of the droplet, $p_c = p(0)$ is the central pressure and the effective surface tension can be computed as $\sigma = -R^{-1} \int_R^\infty r p(r) \mathrm{d}r$. In the large $R$ limit, $p_c = 0$, the gradient term in eq. (3) can be neglected close to the origin, and using eq. (4) we get

$$\int_0^{A_\infty^2} F(U)\mathrm{d}U - A_\infty^2 F(A_\infty^2) = 0, \qquad (5)$$

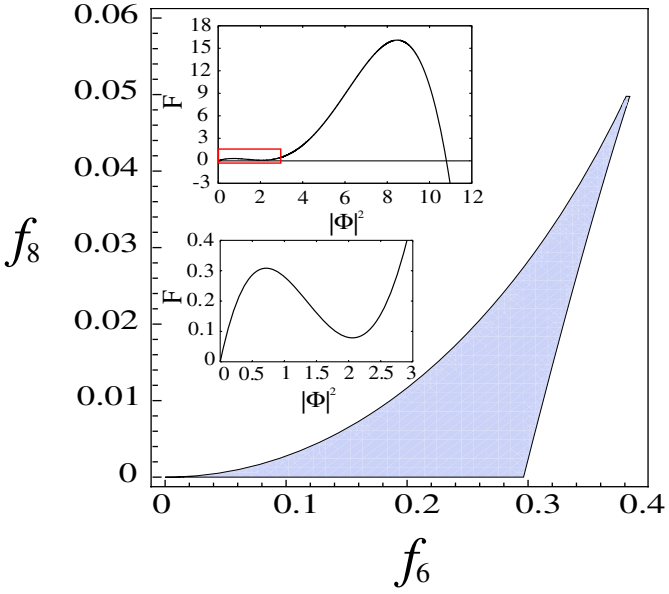


Fig. 1: (Colour on-line) Multistability domain given by eq. (7). Upper inset: nonlinear refractive index correction $F$ as a function of the peak intensity of the light beam $|\Phi|^2$. Lower inset: detail of the region displayed within the red box depicted in the upper inset.

being $\mu_\infty$ and $A_\infty$ the asymptotic values corresponding to the $R \to \infty$ droplet.

In particular, for media whose nonlinear response is described by eq. (2), including terms up to $f_8$, we get the condition

$$\frac{1}{2} - \frac{2}{3}U + f_6 \frac{3}{4}U^2 - f_8 \frac{4}{5}U^3 = 0, \qquad (6)$$

where $U = A_\infty^2$. This cubic equation, giving $f_6$ and $f_8$, can have either one or three real roots. The latter case will eventually correspond to OSM. After a long but straightforward algebra, we get the following necessary and sufficient condition on $f_6$ and $f_8$ for eq. (6) to have three real solutions:

$$18225 f_6^3 - 5400 f_6^2 - 77760 f_6 f_8 + 20480 f_8 + 93312 f_8^2 < 0. \qquad (7)$$

In fig. 1, we plot the region of the $(f_6, f_8)$ plane that satisfies such a condition, assuming $f_6, f_8 > 0$. In particular, for $f_6 > 0.38$ or $f_8 > 0.05$, condition 7 is not fulfilled and only one solution can be found. Conversely, for pairs $(f_6, f_8)$ lying within the shaded region in fig. 1, three different branches of solitons can be found in principle, whose amplitude $A_\infty$ for $R \to \infty$ can be obtained from eq. (6). In the case of oxygen (air), that was examined in ref. [12], $f_6 = 2.8$ and $f_8 = 3.9$ ($f_6 = 11.2$ and $f_8 = 34.1$). These values fall out of the shaded region in fig. 1, and in fact only one branch of solitons was found in ref. [12].

Hereafter, we will fix the values $f_6 = 0.3$ and $f_8 = 0.02$, that lie in the OSM domain, although we have verified that similar results can be obtained for different

choices satisfying eq. (7). The nonlinear refractive index dependence on the intensity of the input beam acquires then a double-hump structure (see insets in fig. 1). In fact, the emergence of OSM can be heuristically related to the appearance of the two maxima of the refractive index, suggesting the possible existence of families of fundamental solitons with limiting intensities close to the values corresponding to the two local maxima of $F$. However, the double-hump structure alone does not guarantee the emergence of OSM, as we have checked by finding values of $(f_6, f_8)$ not satisfying the multistability condition 7, that nevertheless lead to a similar double-peak structure for $F$.

With the choice $f_6 = 0.3$, $f_8 = 0.02$, we calculate the three roots of eq. (7), $A^o_\infty = 1.087$, $A^g_\infty = 1.601$, $A^u_\infty = 3.212$, together with their corresponding values for the propagation constant, as given by eq. (4), $\mu^o_\infty = -0.241$, $\mu^g_\infty = -0.182$, $\mu^u_\infty = -6.72$. The superscripts $o$, $g$, $u$ refer to the names that will be given to the three branches of solitons corresponding to these limiting values, namely *ordinary* solitons, *ghost* solitons and *ultrasolitons*, respectively.

**Localized stationary solutions. Ultrasolitons.** – We have solved eq. (1) numerically, and found the localized stationary states shown in fig. 2. We obtain two different branches of solutions that cannot be connected with each other, *i.e.*, there are no bifurcations in the eigenstates' structure. The red dotted line stands for the *ordinary* soliton branch, *i.e.*, the branch of solutions similar to those reported in [12], whose lower (upper) limit corresponds to the critical power [23] for self-focusing ($A^o_\infty$ plane wave). The presence of HOKE nonlinearities gives rise to a new family of solutions, represented by black lines in fig. 2, whose upper limit corresponds to the $A^u_\infty$ plane wave. Their lower limit does not correspond to the Kerr limit, which means that their existence cannot be explained by a balance between diffraction and the leading Kerr nonlinearity driven by $f_2$, but rather as an interplay between competing HOKE nonlinearities. To our best knowledge, such solutions do not have counterparts in any other nonlinear optical system ruled by local intensity-dependent nonlinearities because they exist over a certain intensity threshold and feature both amplitudes and propagation constants higher (in absolute value) than those of the ordinary ensemble. In other words, these solitons belong to a completely different nonlinear regime as compared with that of the ordinary branch. For all the previous reasons, we have called them *ultrasolitons*. On the other hand, according to the Vakhitov-Kolokolov (VK) criterium [27] supported by systematic simulations of propagation, we find that the eigenstates represented by the solid (dashed) line are dynamically stable (unstable).

The eigenstates b), c) and d), that are represented in the lower-left inset of fig. 2, feature the same optical power but different propagation constants and radial profiles. Analogously, the flat-top eigenstates of insets e) and f) also correspond to the same power, thus

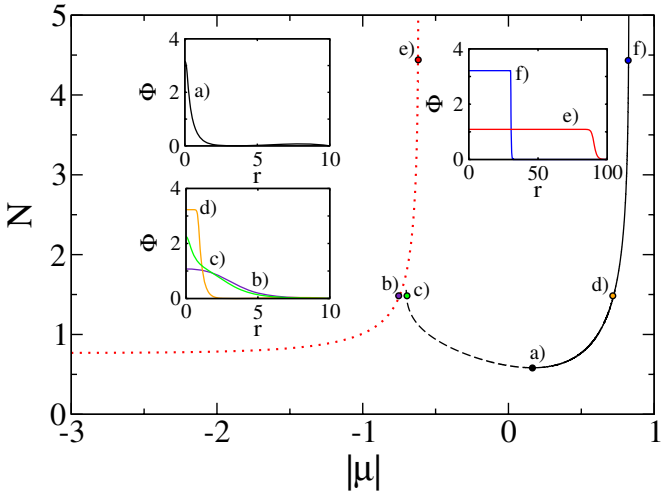


Fig. 2: (Colour on-line) Optical power $N$ *vs.* propagation constant $|\mu|$ for the localized nodeless stationary states of the system described by eq. (1). Both axes display logarithmic scales. The red dotted (black solid) line stands for stable ordinary solitons (ultrasolitons), while the black dashed line stands for unstable ultrasolitons. Labeled points on the main curves refer to the eigenstates displayed within the insets. Insets: radial profiles of several eigenstates of the system, whose propagation constants are $\mu_a = -1.46 =$, $\mu_b = -0.18$, $\mu_c = -0.20$, $\mu_d = -5.26$, $\mu_e = -0.24$ and $\mu_f = -6.67$, respectively. Notice that all solitons depicted within each inset feature the same power $N$, being this a proof of the existence of OSM.

demonstrating OSM even in the high power regime. Both cases demonstrate the emergence of OSM, generalizing to our multibranch situation the definition given in [18] for a single continuous branch.

On the other hand, the solution displayed in inset a) of fig. 2 is the first stable ultrasoliton, and corresponds to a local minimum of the ultrasoliton power curve depicted in fig. 2, being this a trace of the uniqueness of this solution. Very remarkably, this soliton features a *subcritical* power ($N = 3.83$ in dimensionless units), below the ordinary collapse threshold ($N = 5.85$). To our best knowledge, this is the first example of a stable subcritical soliton in an optical system with an instantaneous nonlinear response. Moreover, this minimum power state turns out to have the lowest possible central intensity ($I = 9.98$) among the stable ultrasolitons, although we have found unstable ultrasolitons (corresponding to the dashed curve in fig. 2) starting from central intensities as small as $I = 4.88$.

In fig. 2 we have only plotted two branches of solutions, the ordinary solitons and ultrasolitons. In fact, we have not been able to find numerically the third family of solitary waves linked to the plane wave with amplitude $A^g_\infty$ that we have theoretically predicted above. We can understand its non-existence by using three different arguments.

First, we recall that, according to refs. [12,25], for large but finite flat-topped solutions the central pressure $p_c$ does not vanish, being compensated by the surface tension $\sigma$

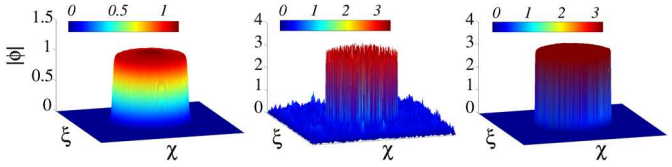


Fig. 3: (Colour on-line) 3D pseudocolour plots of the amplitude of three flat-topped beams modeled by eq. (9) with amplitudes $\Lambda = A^o_\infty$ (left), $A^g_\infty$ (middle), $A^u_\infty$ (right), after a propagation distance of $\eta = 2000, 100$ and 2000, respectively. They have been initially perturbed with a 5% random noise. We see that both beams featuring $A^o_\infty$ and $A^u_\infty$ remain stable while the one having $A^g_\infty$ undergoes filamentation. The spatial scales spanned are $(\xi, \chi) \in [-100, 100]$.

like in an ordinary liquid. The actual values of $\sigma$ for the three branches can be computed as

$$\sigma = \frac{1}{\sqrt{2}} \int_0^{A_\infty} \left( -\mu_\infty A^2 - \sum_{q=1}^{4} (-1)^{q+1} \frac{f_{2q} A^{2(q+1)}}{q+1} \right)^{\frac{1}{2}} \mathrm{d}A. \tag{8}$$

We find: $\sigma^o = 0.0948$, $\sigma^g = 0.0484 + 0.120i$ and $\sigma^u = 7.21$. The fact that for the *ghost* family the surface tension $\sigma^g$ is not real reflects the impossibility of equilibrating the inner pressure, which is a real magnitude, thus forbidding the existence of finite *ghost* solitons. In other words, the ghost solitons would not fulfill the YL equilibrium condition.

Second, we have applied to the plane wave solutions of our system a linear stability analysis similar to that of refs. [28,29]. After a straightforward study, we have found that the solutions with $A^o_\infty, A^u_\infty$ are linearly stable, *i.e.*, they do not undergo modulational instability under small perturbations, while the $A^g_\infty$ lies within an instability window.

Third, we have studied numerically the propagation of three flat-top beams belonging to the high power regime of each of the three branches. The initial condition of our simulations is modeled by the following function:

$$\phi = \Lambda(0.25\{[1 + \tanh(r + \omega)][1 - \tanh(r - \omega)]\}), \tag{9}$$

where $\Lambda = A^o_\infty$, $A^g_\infty$, $A^u_\infty$ is the amplitude of the beam envelope and $\omega = 50$ is the mean radius. We perturb the initial beam profiles with a 5% random noise in order to stimulate the onset of instability. The final states arising from the propagation of such initial conditions are displayed in fig. 3. In the left (right) picture, we show the surface amplitude plot of the flat-top beam having an initial amplitude $\Lambda = A^o_\infty$ ($A^u_\infty$), at a propagation distance $\eta = 2000$. We see that such beam is stable, as it quickly couples to a stable eigenstate of the low-intensity (high-intensity) branch of ordinary solitons (ultrasolitons) discussed above. In the middle picture, we show the outcome of the propagation of an initial beam having $\Lambda = A^g_\infty$, at a propagation distance $\eta = 100$. In this case, we

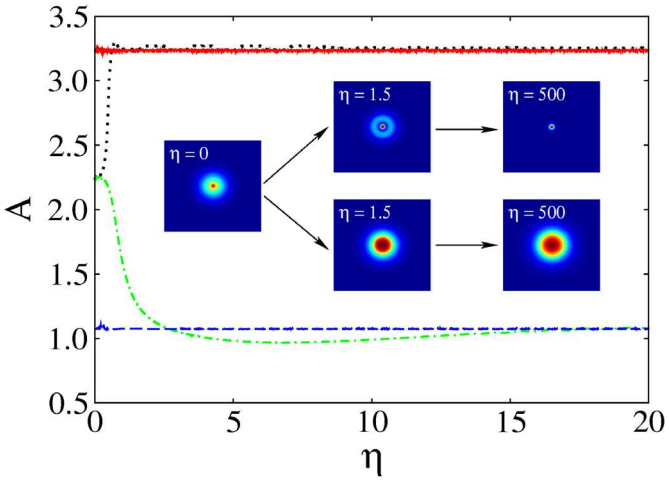


Fig. 4: (Colour on-line) Evolution of the peak amplitude $A = \Phi(0, 0)$ of the eigenstates b) (blue dashed line), c) (green dashed-dotted line) and d) (red solid line) displayed in fig. 2. We observe that both b) and d) fields are stable against small perturbations, while the eigenmode c) becomes unstable, decaying to the lower branch through a soliton switching mechanism. Alternatively, the unstable mode c) can excite a stable ultrasoliton (black dotted line) by adding an initial wavefront curvature to the optical field. The upper (lower) row of inner snapshots show several pseudocolour amplitude plots of the optical field during the soliton switching procedure, where an ultrasoliton (ordinary soliton) is excited from the unstable field c). The square window displayed in the snapshots has a width $\omega_{\xi,\chi} = 25$.

observe how the spatial beam profile has been destabilized by the growth of the perturbations, yielding to multiple filamentation like in the Cubic-Quintic model [29]. The arising filaments correspond to perturbed quasi-stationary ultrasolitons. In this context, the onset of filamentation can be considered as an additional trace of the non-existence of the flat-top soliton with $A \approx A^g_\infty$, although it would not be conclusive if taken alone.

However, our present analysis is not sufficient to exclude that triple stability might be found for a different choice of $f_6$ and $f_8$ within the multistability region of fig. 1.

**Soliton switching.** – The existence of OSM, as shown in fig. 2, suggests the possibility of observing transitions between different multistable states. Such beam-reshaping mechanisms may lead to *soliton switching* processes with a great potential for all-optical communications [20]. In order to study the soliton switching in our system, we have simulated the free propagation of three perturbed solitary waves featuring the radial profiles b), c) and d) of fig. 2. The optical power of these beams is $N \approx 30$. The results of the numerical computations are summarized in fig. 4, plotting the peak amplitude evolution of the eigenstates b) (blue dashed line), c) (green dashed-dotted line) and d) (red solid line). Even though we have added a 5% random noise to their initial profiles, both fields b) and d) remain stable, in agreement with the prediction

of the VK criterium applied to our system. On the other hand, the unstable field c) rapidly decays to a nonlinear mode similar to b), even in the absence of external random noise. The conversion efficiency between both modes, measured as the ratio between the optical powers of the fields, is above 90%.

We have observed that the unstable fields always decay to the lower branch (*down-switching*), while the *up-switching* to the ultrasolitons realm does not occur spontaneously. However, we can force such a transition by including a focusing quadratic phase term $e^{-i0.01r^2}$, similar to that introduced by a thin lens. In this case, the unstable beam d) can be promoted to the upper branch (black dotted line in fig. 4) with a maximum conversion efficiency of around 30%, while the energy excess is radiated as a low-intensity reservoir resembling that generated during the excitation of Townes-like waves in air [30]. The difference between the efficiencies of both processes can be understood by mode-coupling arguments. The modal energy transfer becomes more efficient whenever both profiles and phases of the corresponding modes match, and the modes b) and c) of fig. 2 have closer profiles and propagation constants than the modes c) and d). Few stages of the soliton switching process are highlighted in the insets of fig. 4.

**Conclusions.** – We have shown that an optical system involving competing higher-order Kerr nonlinearities can support the existence of power multistability in the absence of any external potential, yielding a new class of solitary waves, called *ultrasolitons*, that may exhibit powers below the ordinary collapse threshold. We have also proposed a mechanism of *soliton switching* for inducing transitions between different multistable nonlinear waves of the system, that could have potential applications in ultrafast optical circuits intended for all-optical communications [20]. We hope that these results will contribute to stimulate the quest for a clarification of the mechanism of ultrashort pulses filamentation.

* * *

DN acknowledges support from the MICINN, Spain, through the FCCI. ACI-PROMOCIONA project (ACI2009-1008). DT thanks the InterTech group at the Universidad Politécnica de Valencia for hospitality during a stay supported by the Government of Spain (PR2010-0415). HM thanks MPQ at Garching for hospitality during his stay supported by "Salvador de Madariaga" program.

REFERENCES

[1] Loriot V., Hertz E., Faucher O. and Lavorel B., *Opt. Express*, **17** (2009) 13429; **18** (2010) 3011(E).
[2] Béjot P., Kasparian J., Henin S., Loriot V., Vieillard T., Hertz E., Faucher O., Lavorel B. and Wolf J.-P., *Phys. Rev. Lett.*, **104** (2010) 103903.
[3] Couairon A. and Mysyrowicz A., *Phys. Rep.*, **441** (2007) 47.
[4] Teleki A., Wright E. M. and Kolesik M., *Phys. Rev. A*, **82** (2010) 065801.
[5] Brée C., Demircan A. and Steinmeyer G., *Phys. Rev. Lett.*, **106** (2011) 183902.
[6] Kolesik M., Mirell D., Diels J. and Moloney J. V., *Opt. Lett.*, **35** (2010) 3685.
[7] Polynkin P., Kolesik M., Wright E. M. and Moloney J. V., *Phys. Rev. Lett.*, **106** (2011) 153902.
[8] Kosareva O., Daigle J.-F., Panov N., Wang T., Hosseini S., Yuan S., Roy G., Makarov V. and Chin S.-L., *Opt. Lett.*, **36** (2011) 1035.
[9] Béjot P., Hertz E., Kasparian J., Lavorel B., Wolf J.-P. and Faucher O., *Phys. Rev. Lett.*, **106** (2011) 243902.
[10] Wahlstrand J. K., Cheng Y.-H., Chen Y.-H. and Milchberg H. M., *Phys. Rev. Lett.*, **107** (2011) 103901.
[11] Wahlstrand J. K. and Milchberg H. M., *Opt. Lett.*, **36** (2011) 3822.
[12] Novoa D., Michinel H. and Tommasini D., *Phys. Rev. Lett.*, **105** (2010) 203904.
[13] Kolesik M., Wright E. M. and Moloney J. V., *Opt. Lett.*, **35** (2010) 2550.
[14] Kasparian J., Béjot P. and Wolf J.-P., *Opt. Lett.*, **35** (2010) 2795.
[15] Ettoumi W., Petit Y., Kasparian J. and Wolf J.-P., *Opt. Express*, **18** (2010) 6613.
[16] Stegeman G., Papazoglou D. G., Boyd R. and Tzortzakis S., *Opt. Express*, **19** (2011) 6387.
[17] Wang H., Fan C., Zhang P., Qiao C., Zhang J. and Ma H., *J. Opt. Soc. Am. B-Opt. Phys.*, **28** (2011) 2081.
[18] Kaplan A. E., *Phys. Rev. Lett.*, **55** (1985) 1291.
[19] Kaplan A. E., *IEEE J. Quantum Electron.*, **21** (1985) 1538.
[20] Kivshar Y. S. and Agrawal G. P., *Optical Solitons: From Fibers to Photonic Crystals* (Academic Press, San Diego) 2003.
[21] Matuszewski M., *Phys. Rev. A*, **81** (2010) 013820.
[22] Borovkova O. V., Lobanov V. E. and Malomed B. A., *Phys. Rev. A*, **85** (2012) 023845.
[23] Marburger J. H., *Prog. Quantum Electron.*, **4** (1975) 35.
[24] Alexandrescu A., Michinel H. and Pérez-García V. M., *Phys. Rev. A*, **79** (2009) 013833; Michinel H., Paz-Alonso M. J. and Pérez-García V. M., *Phys. Rev. Lett.*, **96** (2006) 023903.
[25] Novoa D., Michinel H. and Tommasini D., *Phys. Rev. Lett.*, **103** (2009) 023903.
[26] Landau L. D. and Lifshitz E. M., *Statistical Physics* (Pergamon, Oxford) 1984.
[27] Vakhitov N. G. and Kolokolov A. A., *Radiophys. Quantum Electron.*, **16** (1973) 783.
[28] Bespalov V. I. and Talanov V. I., *JETP Lett.*, **3** (1966) 307.
[29] Novoa D., Michinel H., Tommasini D. and Carpentier A. V., *Phys. Rev. A*, **81** (2010) 043842.
[30] Ruiz C., San-Román J., Méndez C., Díaz V., Plaja L., Arias I. and Roso L., *Phys. Rev. Lett.*, **95** (2005) 053905.